Performance Enhancement of Surface Plasmon Resonance (SPR) Structure Using a Sinusoidal Diffraction Grating

Manish Jangid, Ankur Saharia, Nitesh Mudgal, Sajai Vir Singh, and Ghanshyam Singh

Abstract In this paper, a sinusoidal diffraction grating is being used for designing a Surface Plasmon Resonance (SPR) structure. The operation of the structure has been examined by using the wavelength-interrogation technique. We have considered the reflected amplitude and absorption dip of the SPR response curve as design parameters for designing this structure. On the performance comparison of gold (Au)-based over silver (Ag)-based SPR structure, although the Ag-based SPR structure gives better results. Due to the poor chemical stability of silver, a thin film of gold is used over it which enhances the performance of the proposed bimetallic SPR structure. This can be used in bioscience for observing the variation of refractive index in an analyte.

Keywords Surface Plasmon Resonance · Sinusoidal grating · FDTD simulation · Refractive index · Oxidation · And reflectivity

1 Introduction

Nowadays, SPR-based biosensor attracts more attention. In 1902, when a polarized light was illuminated by wood onto a diffraction grating, Surface Plasmon Waves (SPW) were observed for the first time [1]. A coupling method for Surface Plasmon excitation based on attenuated total reflection (ATR) was proposed [2]. Kretschmann [3] reported the well-known method named as Kretschmann configuration of ATR coupling for SPR sensors. Later on, the grating-based SPR sensors came into the picture due to their easy designing, miniaturization, and integration features. In 1983, the first application of SPR-based biosensor in gas sensing received more attention from researchers [4]. Sensing a small variation in the refractive index(RI) provides

M. Jangid (✉) · A. Saharia · Nitesh Mudgal · G. Singh
Department of Electronics and Communication, Malaviya National Institute of Technology Jaipur, Jaipur 302017, India
e-mail: 2018pwc5345@mnit.ac.in

S. V. Singh
Department of Electronics and Communication Engineering, Jaypee Institute of Information Technology Noida, Noida 201309, India

M. Tiwari et al. (eds.), *Optical and Wireless Technologies*, Lecture Notes in Electrical Engineering 771, https://doi.org/10.1007/978-981-16-2818-4_13

a better way to characterize gases, chemical molecules, and living cells, showing advantages of real-time and label-free detection [5–8]. Because the SPW vector is greater than the free space vector, so to fulfill the requirement of high index profile for excitation of SPR, we need the high index optical structure like a prism [9, 10], patterned nanostructures like diffraction grating [11, 12] or optical fibers [13–18]. In the past two decades, study interests in SPRs have been emerging very fastly, and a large number of practical applications particularly on biosensing are in progress to develop, for example, affinity, kinetics of bio-molecular interaction, specificity, concentration of an analyte, etc. [19] (Fig. 1).

The phenomenon of an SPR is caused when a p-polarized light vector is guided into a smooth, rough, or grating thin metal surface like silver, gold, and aluminum, etc. (Fig. 2).

The free electrons near such surface collectively oscillate, and an SPW propagates at metal–dielectric interface. At the resonant condition, most of the part of light is coupled, and only small amounts of light loss is observed; a sharply reflected signal is being observed in intensity profile. The required e-field components corresponding to SPW should be p-polarized light because the metal layer and oscillations of e-field vector both are the same in-plane.

These resonance characteristics of SPR spectra (sensogram) provide information about surface (metal-dielectric) interactions in a real-time monitoring system [22]. The SPR sensors can be categorized based on wavelength-interrogation, angle-interrogation, intensity-interrogation, phase-interrogation, and polarization-interrogation techniques [23].

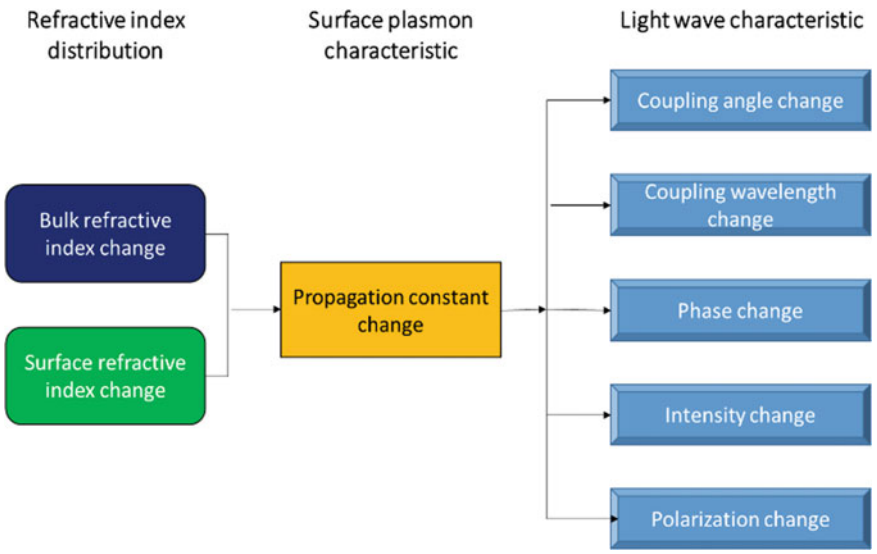

Fig. 1 Concept of SPR sensors. Reproduced from [20]

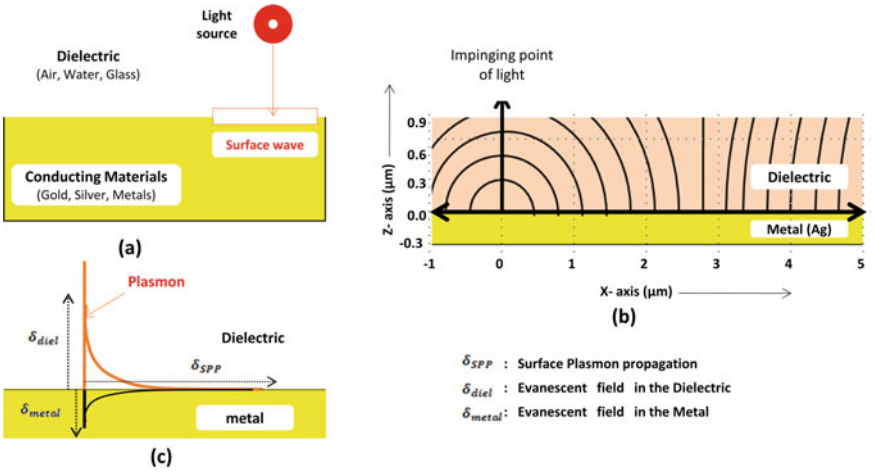

Fig. 2 **a** Condition for SPR occurrence, **b** TM electromagnetic wave guided between metal and dielectric interface. **c** Evanescent field and SPP distribution. Reproduced from [21]

For the evaluation of SPR sensor performance, metal's dielectric constant plays a vital role. Here, the performance of gold (Au) and silver (Ag)-based SPR structure was compared and found that silver-based SPR structure has better performance over the gold-based structure. In the end, to eliminate oxidation problem that arose in silver-based structure, a thin gold film is layered on its surface.

2 Mathematical Modeling

The condition of SPR condition occurs only at the boundary of two different mediums having opposite dielectric constants in nature [24]. A simple SPR contains a metal layer and has a permittivity of $\epsilon_{\text{metal}} = \epsilon'_{\text{metal}} + \text{i}\epsilon'_{\text{metal}}$ and a dielectric layer with a permittivity $\epsilon_{\text{diel}} = \epsilon'_{\text{diel}} + \text{i}\epsilon'_{\text{diel}}$ [8]. SPW has a property of an evanescent wave containing maximum magnetic field intensity at the metal–dielectric interface and decaying into both the medium [6]. SPW is a transverse-magnetic (TM) wave in nature, guided between metal and dielectric interface [25]. The Surface Plasmon's Wave vector $\left(K_{\text{Sp}}\right)$ can be expressed for the metal–dielectric interface as

$$K_{\text{Sp}} = \frac{2\pi}{\lambda}\sqrt{\frac{\epsilon_{\text{diel}}\,\epsilon_{\text{metal}}}{\epsilon_{\text{diel}} + \epsilon_{\text{metal}}}} \tag{1}$$

where dielectric constant for metal is ϵ_{metal} and for the dielectric layer is given by ϵ_{diel}. The incident light vector is generally less than SPW vector, which is defined as $k_\alpha = \frac{2\pi}{\lambda} n_x \sin\theta_x$ (Refractive Index of an analyte is n_x and the angle in the analyte

is θ_x). In the coupling mechanism of grating, the diffracted light beam vector (k_β) is the sum of k_α and the grating wave vector [7, 26].

$$k_\beta = k_\alpha + \gamma \frac{2\pi}{P} \tag{2}$$

where diffraction order γ is an integer number and P is grating constant. So, now SPR excitation condition can be expressed as $k_\beta = k_{\text{sp}}$, which is written as

$$n_x \sin\theta_x n_x + \gamma \frac{\lambda}{P} \pm = \sqrt{\frac{n_x^2 \epsilon_{\text{metal}}}{n_x^2 + \epsilon_{\text{metal}}}} \tag{3}$$

Here, ϵ_{diel} is replaced by n_x^2, the sign ' $\pm$ ' shows the propagation of Surface Plasmon along the positive or negative direction.

Silver and gold are preferably used metals for the designing of SPR sensors since they exhibit a narrow resonance curve [27]. Based on these two metals, SPR structure's performance is analyzed. Lorentz–Drude equation [28] is used to calculate the value of ϵ_{metal}.

$$\epsilon_{\text{metal}}(\omega) = 1 - \frac{\varphi_p^2}{\omega(\omega - i\Gamma_{0)}} \tag{4}$$

where $\omega = \frac{2\pi c}{\lambda}$ and $\varphi_P = \sqrt{f_0 \omega_P}$ is the plasma frequency, f_0 is the oscillator strength, and Γ_0 is the damping constant. The values of f_0, ω_P, and Γ_0 are calculated from [29, 30].

3 Designing and Simulation

A schematic for designing the proposed SPR structure using sinusoidal grating is shown in Fig. 3. Grating thickness (g), constant/period (p), and substrate thickness (t) are being considered as constructor parameters for designing the proposed SPR structure. The wavelength-interrogation-based performance of SPR sensor can be calculated by resonance wavelength shift and absorption dip of reflected signal in the SPR response spectra. The amplitude of reflected signal and resonance wavelength shifts and must be significantly large for observing a distinctive and high precision signal.

Figure 4a states the reflection curve of silver (Ag)-based SPR structure for grating constants $p1 = 800$ nm and $p2 = 1000$ nm. The other parametric values of the structure are grating thickness (g) = 50 nm, substrate thickness (t) = 40 nm. Here, the wavelength of 633 nm is being used as a guiding light signal. In Fig. 4a, we observed that the grating period/constant (p) increases from 800 to 1000 nm, and the resonance

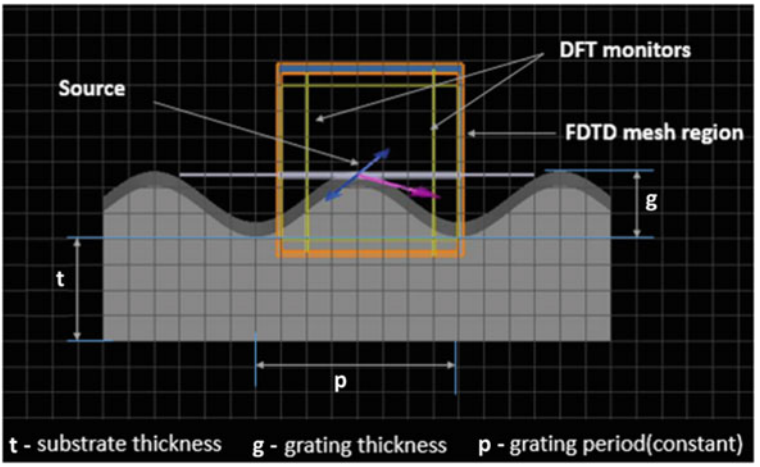

Fig. 3 Schematic diagram of a sinusoidal diffraction grating-based SPR sensor

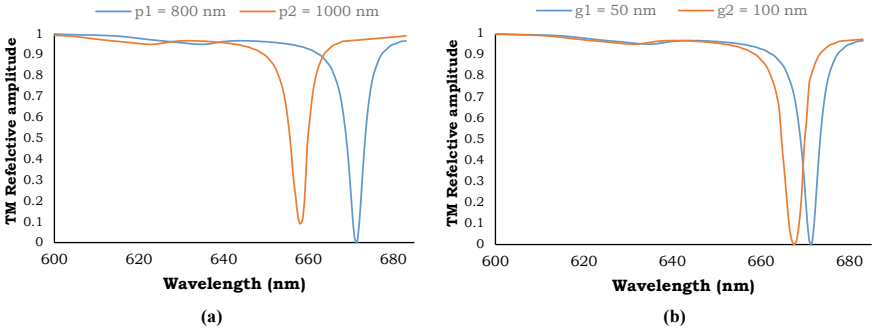

Fig. 4 **a** Reflection curve of silver (Ag) based SPR structure for grating constants $p1 = 800$ nm and $p2 = 1000$ nm. **b** Reflection curve of silver (Ag) based SPR structure for grating thicknesses $g1 = 50$ nm and $g2 = 100$ nm

wavelength's amplitude decreases. So, we selected the grating constant $p = 800$ nm as an optimal value. It was observed that as the grating constant was increased, the reflectance dips of the SPR response curve also rose. For better performance of SPR structure, we need a larger reflectance dip of the SPR response curve. Similarly, Fig. 4b displays the reflection curve of silver (Ag)-based SPR structure for grating thicknesses $g1 = 50$ nm and $g2 = 100$ nm. It is clear that at 50 nm grating thickness SPR, we got the smallest SPR dip along with the smallest reflected amplitude at $g = 30$ nm. But when $g = 100$ nm, the SPR dip observed was wider. Here, it is clear that for optimal performance, the value of grating thickness should lie between 30 and 100 nm. So, when the grating thickness (g) is 50 nm, the reflected amplitude is the highest, and the SPR dip is also very small

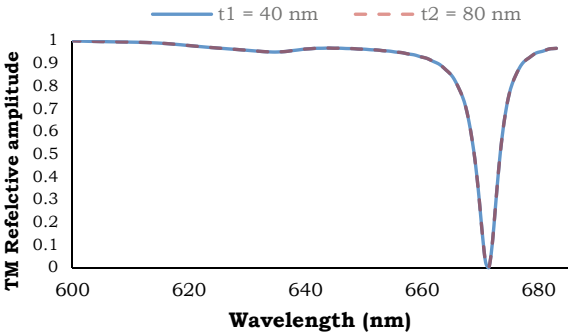

Fig. 5 Reflection curve of silver (Ag) based SPR structure for substrate thicknesses $t1 = 40$ nm and $t2 = 80$ nm

This is the condition, where the maximum light of incident wave is being coupled. Therefore, based on the above consideration, we selected the grating thickness (g) = 50 nm as optimal value.

Figure 5 illustrates the reflection curve of silver (Ag)-based SPR structure for grating substrate thickness $t1 = 40$ nm and $t2 = 80$ nm. The light is launched onto the grating surface vertically. By considering the substrate thickness (t) below 40 nm, the reflected amplitude observed was small as compared to the 40 nm thickness. Similarly, on increasing the substrate thickness beyond the 40 nm, there was no variation observed in reflected amplitudes of the SPR dips. Hence, the substrate thickness (t) = 40 nm provides better performance for proposed structure

Figure 6a states the reflection curve of gold (Au)-based SPR structure for grating constants $p1 = 800$ nm and $p2 = 1000$ nm. The parametric values of the structure are the same as a silver-based sensor, grating thickness (g) = 50 nm, and substrate thickness (t) = 40 nm. As the grating period/constant was increased from 800 to 1000 nm, the resonance wavelength decreased. It was observed that as the grating constant was increased, the reflectance dips of the SPR response curve also rose. Since we needed a larger reflectance amplitude, so we selected grating constant (p) = 800 nm as optimal value. Figure 6b displays the simulated reflection spectra of gold (Au)-based SPR structure for grating thicknesses $g1 = 50$ nm and $g2 = 100$ nm.

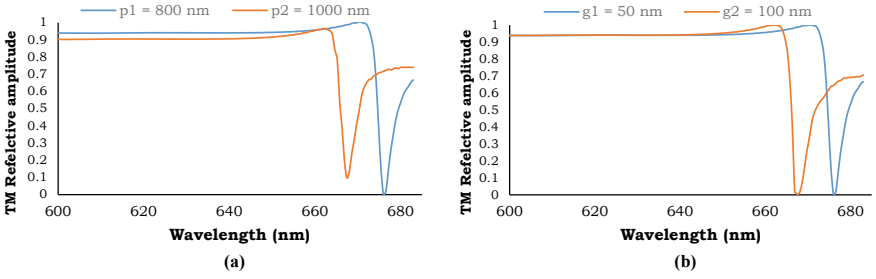

Fig. 6 **a** Reflection curve of gold (Au) based SPR structure for grating constants $p1 = 800$ nm and $p2 = 1000$ nm. **b** Reflection curve of gold (Au)-based SPR structure for grating thicknesses $g1 = 50$ nm and $g2 = 100$ nm

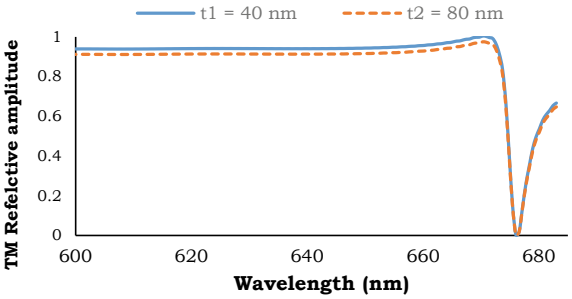

Fig. 7 Reflection curve of gold (Au)-based SPR structure for substrate thicknesses $t1 = 40$ nm and $t2 = 80$ nm

It was observed that below 50 nm and on and beyond 100 nm grating thickness, the SPR response curve did not meet the requirement. At grating thickness $(g) = 50$ nm, the maximum incident light coupled with SPW

Figure 7 illustrates the reflection curve of gold (Au)-based SPR structure for grating substrate thickness $t1 = 40$ nm and $t2 = 80$ nm. The best performance of Au-based structure was observed at substrate thickness $(t) = 40$ nm. Here, we observed that the gold-based structure has a wider resonance dip than a silver-based structure

But we require a sharp resonance dip as per the requirement of a high-performance SPR sensor. So, we suggested a bimetallic gold (Au)–silver (Ag)-based structure and simulated under the same parametric values.

The wavelength SPR curves of the Ag-based sensor and Au-based sensor are illustrated corresponding in Fig. 8a, b. It clearly witnessed that as the RI of the analyte n_a increases, the reflectance dips move gradually to the leftward. It can be evidenced that the reflectance dip value of gold-based sensor analogous to the resonance wavelength is higher than that of silver-based sensor. Since at resonant wavelength, silver offers the lower reflectance dip compared with gold, so we consider that silver-based sensor exhibits superior resonance performance. We got the sensitivities of 890.26 nm/RIU for silver-based and 646.74 nm/RIU for gold-based sensor. It clearly states that the silver-based sensor has larger sensitivity than gold-based sensor. But, there is problem

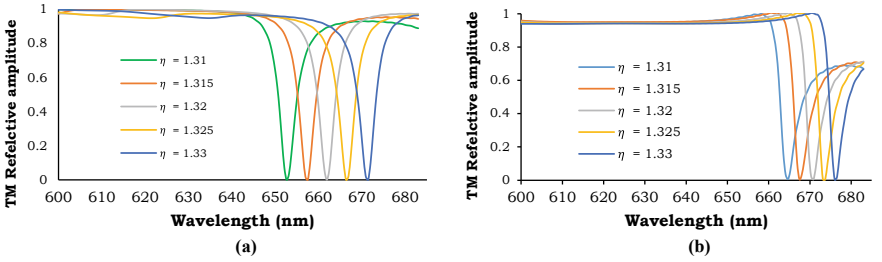

Fig. 8 **a** Wavelength SPR curves for silver-based SPR structure. The RI of an analyte ranging from 1.31 to 1.33. **b** Wavelength SPR curves for gold-based SPR structure. The RI of an analyte ranging from 1.31 to 1.33

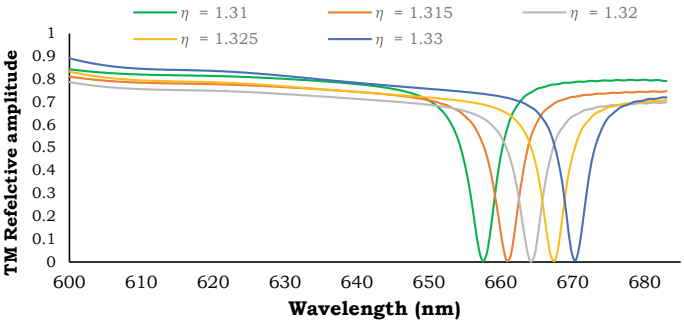

Fig. 9 Wavelength SPR curves for bimetallic SPR structure. The RI of an analyte ranging from 1.31 to 1.33

associate with silver metal, i.e., oxidation. This kind of problem decreases the durability and reliability of such SPR structure. That's why, a bimetallic gold (Au)–silver (Ag)-based structure is suggested and simulated under the same parametric values. In designing perspective, a bimetallic structure is construct with an Ag-layer of thickness 47 nm and an Au- layer (as a protective layer) of thickness 3 nm over it, which practically enhances the durability of this SPR sensor.

The SPR curve for bimetallic-based sensor illustrates in Fig. 9. The bimetallic SPR curve is almost similar to the Ag-based SPR structure as depicted in Fig. 8a. The sensitivity of bimetallic SPR sensor is 842.28 nm/RIU. This value is small to some extent that of Ag-based sensor. Results show that there is no significant difference in the sensitivity of the silver-based SPR structure compared to the bimetal SPR structure. Both sensitivities values are quite similar.

Here the proposed bimetallic SPR structure is better in reliability point of view as compared to silver SPR structure. Here we observed minimum reflectivity of proposed SPR structure that indicates that maximum light is being coupled and also enhances the efficiency of SPR structure.

4 Conclusion

A practical simulation of a SPR-based sensor is done in this research work to witness the impact of silver and gold thin metal's film on the performance parameters of the proposed structure. The investigation was performed using a reflectivity graph which provide the information about the shift in Plasmon dip of coupled optical signal at a particular angle of incidence. Subsequently, a numerical investigation was performed that reflected the influence of structural parameters on the performance analysis of proposed SPR biosensor. The effect of sinusoidal grating on the output of the proposed SPR was assessed by varying the grating thickness, grating constant, and thickness of the substrates. For optimized values of grating's design parameters,

the shift of the Plasmon wavelength was determined. The main feature of this SPR biosensor is the use of sinusoidal bimetallic (gold–silver) grating to improve the quality of the SPR signals. The RI dynamic range of this sensor ranges from 1.31 to 1.33 and has the highest sensitivity (842.28 nm/RIU). We have ensured minimum possible reflectivity with maximum sensitivity in this proposed biosensor.

References

1. Jamil NA, Menon PS, Said FA, Tarumaraja KA, Mei GS, Majlis BY (2017) Proc IEEE Reg Symp Micro Nanoelectron RSM 2017:112–115
2. Wood RW (1902) On a remarkable case of uneven distribution of light in a diffraction grating spectrum. Lond Edinb Dublin Philos Mag J Sci 4:396–402
3. Otto A (1968) Excitation of nonradiative surface plasma waves in silver by the method of frustrated total reflection. Zeitschrift für Physik A Hadrons and Nuclei 216:398–410
4. Kretschmann E (1996) Determination of optical constants of metals by excitation of surface plasmon sensing. Sens Actuators B Chem 35:212
5. Liedberg B, Nylander C, Lunström I (1983) Surface plasmon resonance for gas detection and biosensing. Sens Actuators 4:299–304
6. Homola J, Yee SS, Gauglitz G (1994) surface plasmon resonance sensors: review. Sens Actuators B 54:3–15
7. Wijaya E, Lenaerts C, Maricot S, Hastanin J, Habraken S, Vilcot JP, Boukherroub R, Szunerits S (2011) Surface plasmon resonance-based biosensors: from the development of different SPR structures to novel surface functionalization strategies. Curr Opin Solid State Mater Sci 15:208–224
8. Homola J (2008) Surface plasmon resonance sensors for detection of chemical and biological species. Chem Rev 108:462–493
9. Tong L, Wei H, Zhang S, Xu H (2014) Recent advances in plasmonic sensors. Sensors 14:7959–7973
10. Kretschmann E, Raether H (1968) Radiative decay of non-radiative surface plasmons excited by light. Z Naturforsch 23A:2135–2136
11. Otto A (1968) Excitation of nonradiative surface plasma waves in silver by the method of frustrated total reflection. Z Phys A Hadron Nuclei 216:398–410
12. Cullen DC, Brown RG, Lowe CR (1987) Detection of immuno-complex formation via surface plasmon resonance on gold-coated diffraction gratings. Biosensors 3:211–225
13. Jory MJ, Vukusic PS, Sambles JR Development of a prototype gas sensor using surface plasmon resonance on gratings. Sens. Actuators B Chem
14. Bhatia P, Gupta BD (2011) Surface-plasmon-resonance-based fiber-optic refractive index sensor: sensitivity enhancement. Appl Opt 50:2032–2036
15. Bhatia P, Gupta BD (2013) Surface plasmon resonance based fiber optic refractive index sensor utilizing silicon layer: effect of doping. Opt Commun 286:171–175
16. Singh S, Mishra SK, Gupta BD (2013) Sensitivity enhancement of a surface plasmon resonance-based fiber optic refractive index sensor utilizing an additional layer of oxides. Sens Actuators A Phys 193:136–140
17. Tabassum R, Gupta BD (2015) Performance analysis of bimetallic layer with zinc oxide for SPR-based fiber optic sensor. J Lightw Technol 33:4565–4571
18. Tabassum R, Gupta BD (2017) Influence of oxide overlayer on the performance of a fiber optic SPR sensor with Al/Cu layers. IEEE J Sel Top Quantum Electron 23:81–88
19. Usha SP, Gupta BD (2017) Performance analysis of zinc oxide-implemented lossy mode resonance-based optical fiber refractive index sensor utilizing thin-film/nanostructure. Appl Opt 56:5716–5725

20. Homola J, M Piliarik (2006) Surface plasmon resonance (SPR) sensors. Ser Chem Sens Biosens 4:45–67
21. Reports on progress in physics. IOPscience 75:036501 (2012)
22. Liedberg B, Lundstrom I, Stenberg E (1993) Principles of biosensing with an extended coupling matrix and surface plasmon resonance. Sens Actuators B Chem 11(1–3):63–72
23. Homola J (2003) Anal Bioanal Chem 377:528
24. Schasfoort RB (2017) Handbook of surface plasmon resonance. Royal Society of Chemistry, Cambridge, UK
25. Homola J, Koudela I et al (1999) Surface plasmon resonance sensors based on diffraction gratings and prism couplers: sensitivity comparison. Sens Actuators B 54:16–24
26. Homola J (1997) On the sensitivity of surface plasmon resonance sensors with spectral interrogation. Sens Actuators B Chem 41:207–211
27. Byun KM, Kim SJ et al (2007) Grating-coupled transmission-type surface plasmon resonance sensors based on dielectric and metallic gratings. Appl Opt 46:5703–5708
28. Ung B, Sheng Y (2007) Interference of surface waves in a metallic nanoslit. Opt Expr 15:1182–1190
29. Rakić AD, Djurišić AB, Elazar JM, Majewski ML (1998) Optical properties of metallic films for vertical-cavity optoelectronic devices. Appl Opt 37:5271–5283
30. Ung B, Sheng Y (2007) Interference of surface waves in a metallic nanoslit. Opt Express 15:1182–1190